DIRECT ESTIMATION OF THE SEISMIC DEMAND AND CAPACITY OF OSCILLATORS WITH MULTI-LINEAR STATIC PUSHOVERS THROUGH INCREMENTAL DYNAMIC ANALYSIS

Dimitrios Vamvatsikos[1] and C.Allin Cornell[2]

ABSTRACT

The seismic behavior of numerous single-degree-of-freedom (SDOF) systems is investigated through Incremental Dynamic Analysis (IDA), a computer-intensive procedure that offers thorough (demand and capacity) prediction capability by using a series of nonlinear dynamic analyses under a suitably scaled suite of ground motion records. The oscillators are of moderate period with pinching hysteresis and feature backbones ranging from simple bilinear to complex quadrilinear with an elastic, a hardening and a negative-stiffness segment plus a final residual plateau that terminates with a drop to zero strength. The results of the analysis are summarized into their 16%, 50% and 84% fractile IDA curves which are in turn fitted by flexible parametric equations. The final product is SPO2IDA, an accurate, spreadsheet-level tool for Performance-Based Earthquake Engineering that is available on the web. It offers effectively instantaneous estimation of demands and global-instability collapse capacities, in addition to conventional strength reduction *R*-factors and inelastic displacement ratios, for any SDOF system whose Static Pushover curve can be approximated by such a quadrilinear backbone.

Introduction

Of great interest in Performance-Based Earthquake Engineering (PBEE) is the accurate estimation of the seismic demand and capacity of structures. To accomplish the task several important methods have emerged, a promising one being Incremental Dynamic Analysis (IDA), a parametric analysis method that estimates seismic demand and capacity by subjecting the structural model to several ground motion records, each scaled to multiple levels of intensity (Vamvatsikos , 2002a). Still, the need for simplified methods for professional practice remains, and the rational choice has often been the use of results stemming from the dynamic analysis of single-degree-of-freedom (SDOF) approximations to the multi-degree-of-freedom (MDOF) structural model. Such methods often use an oscillator with a backbone curve that mimics the Static Pushover (SPO, also known as Nonlinear Static Procedure) curve of the MDOF structure (e.g., FEMA, 1997). However, most systematic demand research efforts have not progressed further than using an oscillator with a bilinear backbone, allowing only for either positive (Nassar, 1991) or negative (Al-Sulaimani, 1985) post-yield stiffness or, still more simply, elastic perfectly-plastic behavior (Miranda, 2000), while few, if any, attempts have been made to quantify its dynamic, global-instability collapse capacity (e.g., FEMA, 2000). As an extension to existing procedures, it is only natural to apply the IDA method to SDOF systems featuring a variety of backbones and to attempt to quantify the resulting demands and capacities in a handful of comparatively simple empirical equations.

[1]Graduate Student, Department of Civil and Environmental Engineering, Stanford University, CA 94305-4020
[2]Professor, Department of Civil and Environmental Engineering, Stanford University, CA 94305-4020

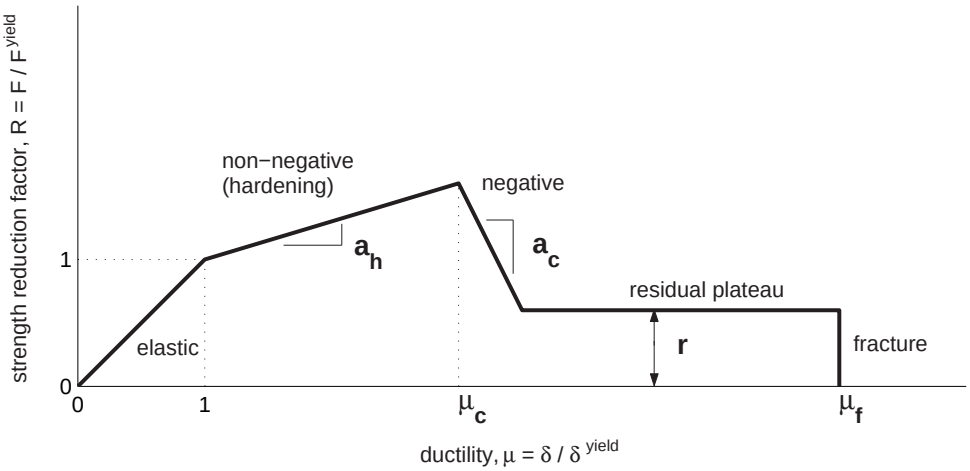

Figure 1. The backbone to be investigated and its five controlling parameters.

Methodology

To study the influence of the SPO curve on the dynamic behavior, we have chosen a piecewise linear backbone that is composed of up to four segments (Fig. 1). A full quadrilinear backbone starts elastically, yields at ductility $\mu = 1$ and hardens at a slope $a_h \in [0,1)$, then at ductility $\mu_c \in (1,+\infty)$ turns negative at a slope $a_c \in [-\infty,0)$, but is revived at $\mu_r = \mu_c + (1-r+(\mu_c-1)a_h)/|a_c|$ by a residual plateau of height $r \in [0,1]$, only to fracture and drop to zero strength at $\mu_f \in [1,+\infty)$. By suitably varying the five parameters, a_h, μ_c, a_c, r and μ_f, almost any (bilinear, trilinear or quadrilinear) shape of the SPO curve may easily be matched.

To fully investigate the dynamic behavior of a single SDOF model, we will use IDA for a suite of thirty ground motion records (Vamvatsikos , 2002b) that have been selected to represent a scenario earthquake; the moment magnitude is within the range of 6.5 – 6.9, they have all been recorded on firm soil (USGS type C or B) and show no directivity effects. IDA involves performing a series of nonlinear dynamic analyses for each record by scaling it to several levels of intensity that are suitably selected to uncover the full range of the model's behavior: elastic, yielding, nonlinear inelastic and finally global dynamic instability. Each dynamic analysis can be represented by at least two scalars, an Intensity Measure (*IM*), which corresponds to the scaling factor of the record (e.g., the strength reduction factor $R = S_a(T_1,5\%)/S_a^{\text{yield}}(T_1,5\%)$, which is equal to the 5%-damped first-mode spectral acceleration $S_a(T_1,5\%)$ normalized by its value that causes first yield) and a Damage Measure (*DM*), which monitors the structural response of the model (e.g., peak ductility μ).

By suitably interpolating between the runs that were performed for a given record, we can plot on the *DM*-*IM* axes an IDA curve for each record, e.g., Fig. 2(a). Each curve ends with a characteristic "flatline" which indicates that the *DM* rapidly increases towards "infinite" values for small changes in the *IM*, thus signalling global dynamic instability and defining the global-collapse capacity at the *IM* where the IDA curve effectively becomes flat. Such "capacity points" are visible as black dots in Fig. 2(a). A set of IDA curves can be summarized into 16%, 50% and 84% cross-sectional fractile IDAs of response μ given the intensity R or R given μ, depending on how the cross-sections of the curves are taken, e.g., at specified levels of R or μ (Vamvatsikos ,

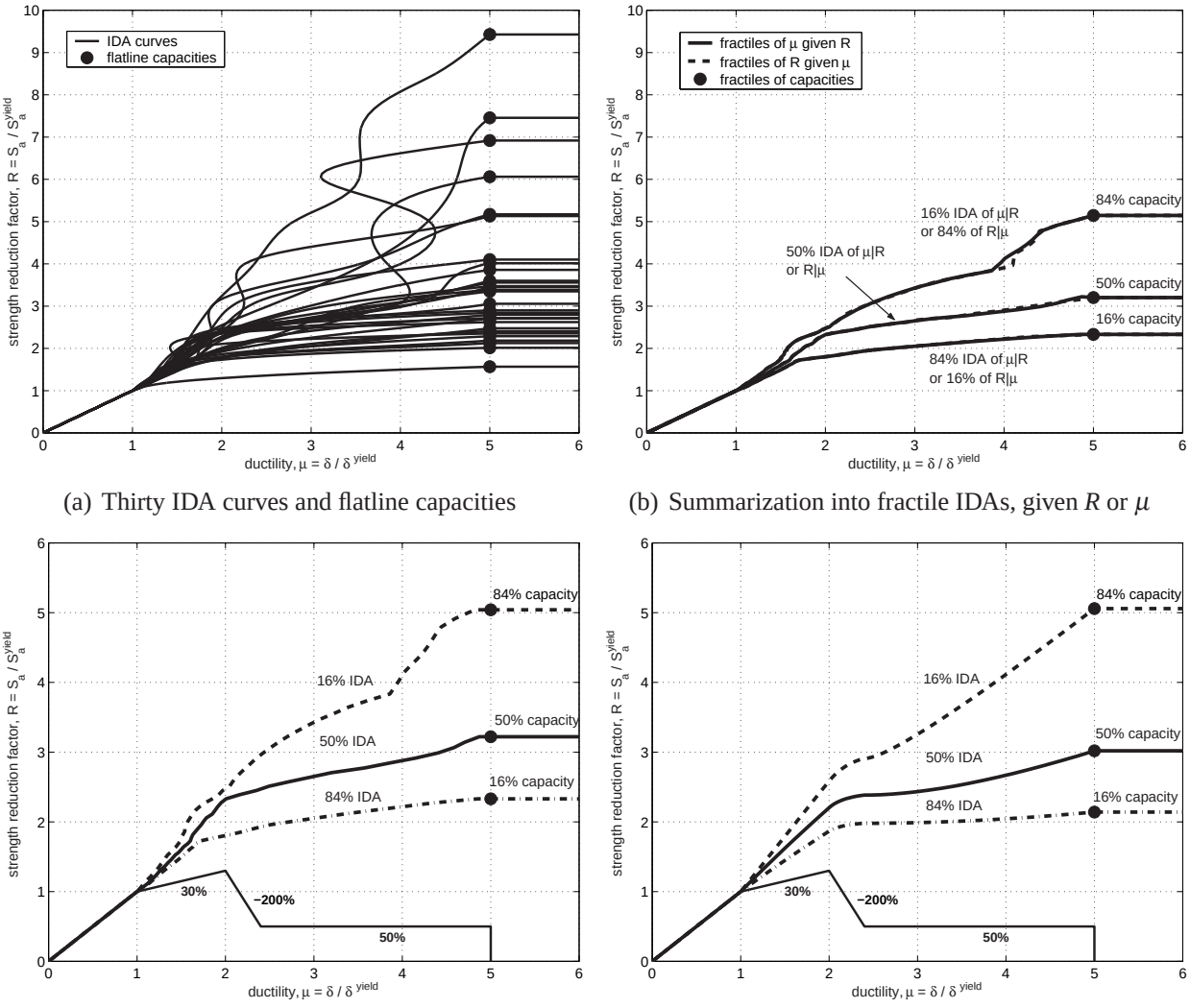

(a) Thirty IDA curves and flatline capacities

(b) Summarization into fractile IDAs, given R or μ

(c) The fractile IDAs from (b) versus the SPO curve

(d) The fractile IDAs, as estimated by SPO2IDA

Figure 2. Generating the fractile IDA curves and capacities from dynamic analyses versus estimating them by SPO2IDA for an SPO with $a_h = 0.3$, $\mu_c = 2$, $a_c = -2$, $r = 0.5$, $\mu_f = 5$.

2002a). Fortunately, under suitable assumptions of continuity and monotonicity, the x%-fractile IDA $\mu_{x\%}(R)$ ($x \in \{16, 50, 84\}$) of μ given R, will be identical (or nearly identical if the assumptions are slightly violated) to the $R_{(100-x\%)}(\mu)$ fractile IDA of R given μ as shown in Fig. 2(b). As a direct result, if we similarly summarize the capacity points, the $(100-x\%)$ global-instability collapse capacity will always appear on the flatline of the x%-fractile IDA of μ given R (Fig. 2(c)).

If we choose to plot the SPO of the SDOF system on μ versus $R = F/F^{\text{yield}}$ axes (where F is the total base shear and F^{yield} its value that causes first yield) we can make it appear versus the summarized IDA curves on the same graph (Vamvatsikos , 2002a), as in Fig. 2(c). Such a comparison shows that the SPO and the fractiles are composed of the same number of corresponding and distinguishable segments. Moreover, each segment has its own nature. The elastic segment of the SPO naturally coincides with the elastic IDA region for all three fractiles, while the yielding and hardening of the SPO forces the 16%, 84% IDAs to branch uniformly around the median which ap-

proximately follows the familiar "equal displacement" rule. The SPO's negative stiffness appears as a characteristic flattening of all three IDAs that stops when the residual plateau is activated, causing the "revival" of the IDA curves towards higher R values. Ultimately, all IDA curves submit to the SPO fracturing, thus signaling collapse by producing a flatline (and the corresponding fractile capacity point).

This consistent behavior makes it is possible to approximate each separate segment of the IDA by its prominent features, e.g., the height of the flatline or the slope and intercept of a fitted line. By examining a large enough population of SDOF systems with different shapes of the backbone, we can track the evolution of the features of each segment, and subsequently model them as a function of the SPO parameters. Thus, we are able to generate almost the same fractile IDAs and capacities (within some acceptable tolerance) without needing to repeat the multiple dynamic analyses. This set of rules and equations will be collectively called the SPO2IDA tool, a typical example of its accuracy visible in Fig. 2(d).

However, the complexity of the backbone has forced us to limit the scope of our investigation by choosing SDOF systems that share an identical moderately pinching hysteresis model with no cyclic degradation (Nassar, 1991), viscous damping of $\xi = 5\%$ and a moderate period of $T_1 = 0.92$sec. The results will thus be a good approximation for the moderate period range, while an extension to shorter and longer periods can be found in (Vamvatsikos , 2002b). Still, the full investigation of a five-dimensional space of parameters requires a staggering amount of dynamic analyses, especially since the parameters do not influence the IDAs independently of each other. Nevertheless, there are several facts that allow us to reduce the size of the problem. First, since we are measuring the *peak* ductility, at any given value of μ the IDA will only be influenced by the segments of the SPO backbone that appear at lesser or equal ductilities. This would not be true if we were monitoring, say, permanent deformation. So, in fitting the hardening branch, the negative stiffness is of no consequence, while in fitting the negative branch, the plateau plays no part. Therefore, we can cut the problem into smaller pieces, as we only need to investigate a bilinear elastic-hardening, a trilinear elastic-hardening-negative but still, a full quadrilinear for the plateau. Even then, we may not have to go all the way, even for the plateau. The idea is that some of the SPO parameters may be redundant, so their influence can be summarized in only one or two new parameters which combine them. In effect this means that (for the same damping and period) we are going to search for "equivalent backbones", in the sense that such oscillators would share very similar dynamic behavior in the region of interest, as manifested by their displaying the same fractile IDAs.

When modeling the IDA features we will use least-squares fits of polynomials, either in the linear or in the log-domain. To simplify the expressions to follow, let us define some convenient symbols to represent linear combinations of consecutive powers of a given variable y.

$$P_n(y) = b_0 + b_1 y + b_2 y^2 + \ldots + b_n y^n = \sum_{i=0}^{n} b_i y^i, \qquad \text{(positive integer } n\text{)} \tag{1}$$

$$P_{m;n}(y) = b_m y^m + b_{m+1} y^{m+1} + \ldots + b_{n-1} y^{n-1} + b_n y^n = \sum_{i=m}^{n} b_i y^i, \text{ (integers } m < n\text{)} \tag{2}$$

As a general principle, note that the small record number, the record-to-record variability and the fitting error, combine to introduce some noise which tends to become larger as the ductility

response itself increases. So we will generally fit elaborate models but only as complex as the noise in the IDA results allows. Still, as we try to interpolate as closely as possible given the noise, we are risking eliciting criticism for "overfitting" (in the sense that a simpler model would do only a little worse). The idea is to provide as a complete and objective model as the record-to-record noise allows, and in retrospect observe it and simplify it enough to satisfy the arithmo-phobic users.

Fitting the hardening branch of the IDA

Fitting the hardening part is the easiest task, and actually several attempts have been done in the past (Miranda, 2000; Nassar, 1991), sometimes for a wider variety of parameters (e.g., site conditions, viscous damping) than what we will use here. Since this fit only involves a single parameter, a_h, it is relatively straightforward; we will assume a second-order polynomial model in the log-space to fit the fractile ductilities given R, and subsequently calculate and fit the resulting coefficients for several values of the hardening slope a_h. This procedure produces for each of the three fractile IDAs the following model

$$\ln \mu_{x\%} = \beta_{x\%} \ln R + \gamma_{x\%} \ln^2 R, \qquad R \in (1, R_{(100-x)\%}(\mu_c)] \tag{3}$$
$$\text{where} \quad \beta_{x\%},\, \gamma_{x\%} = P_4(a_h), \quad \text{for any } a_h \in [0, 0.9)$$

where the coefficients can be conveniently found in Table 1. An example of its application is found in Fig. 2(d) for $1 < \mu \leq 2$.

Table 1. Coefficients needed for the IDA hardening part in Eq. (3)

	$\beta_{x\%}$			$\gamma_{x\%}$		
$x\% =$	16%	50%	84%	16%	50%	84%
1	0.6164	0.7132	1.0024	0.1454	0.2928	0.4003
a_h	-0.1697	-0.0415	1.5907	-0.1394	-0.6415	-3.0742
a_h^2	1.3103	1.5158	-7.1722	-0.2576	0.0347	9.7763
a_h^3	-1.9551	-2.5525	10.3472	0.6156	0.9604	-12.8813
a_h^4	1.2201	1.3921	-4.8024	-0.3707	-0.6620	5.8376

The results are actually only little dependant on a_h, especially for low ductilities. So we can roughly approximate the median IDA by the "equal displacement rule" and generate the 16%, 84% fractiles as the edges of a 60%-wide band centered on the median (in the log-space), i.e., $\mu_{(50\pm34)\%}(R) \approx \mu_{50\%}(R)^{1\pm0.3} \approx R^{1\pm0.3}$.

Fitting the negative branch of the IDA

Negative stiffness is found in SPOs of structures such as non-ductile RC frames, braced steel frames, moment-resisting steel frames with fracturing connections and P-Δ sensitive systems. The most prominent feature of the negative branch is the characteristic flattening of the summarized IDAs which results in a flatline unless it is arrested by the residual plateau, as seen in Fig. 2(c), for $2 < \mu \leq 2.4$. By accurately capturing this feature, the entire branch could be modeled as a continuous convex curve that smoothly departs from the hardening segment at ductility μ_c to blend into

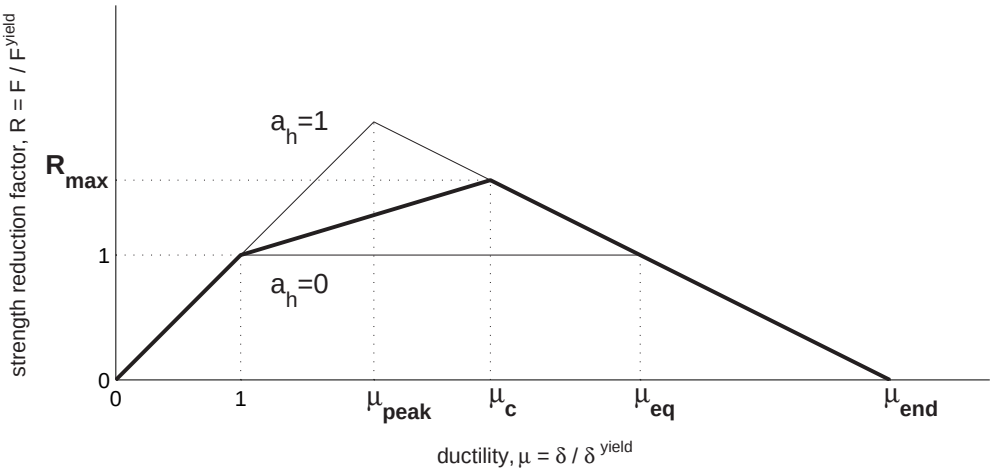

Figure 3. An elastic-hardening-negative backbone and the two extremes of its "equivalent" set.

the flatline at $\mu_{\text{end}} = \mu_c + (1 + a_h\mu_c - a_h)/|a_c|$. Still, appropriately modeling the negative branch flatline requires a trilinear (elastic-hardening-negative) backbone that involves three independent parameters (a_c, a_h and μ_c). Conveniently enough, it was found empirically that this flatline height and, even more, the complete negative part of the IDA are very similar for the set of backbones that have coincident negative branches, like those in Fig. 3. Actually, the flatline height among such an equivalent set varies only a little and always in a consistent monotonically increasing fashion between the two extremes, i.e., the $a_h = 0$ and the $a_h = 1$ cases where the negative branch starts at $\mu_{eq} = \mu_c + a_h(\mu_c - 1)/|a_c|$, and $\mu_{peak} = (\mu_c|a_c| + 1 + a_h(\mu_c - 1))/(1 + |a_c|)$ respectively. So we only need to model the capacities for the extreme values of a_h and linearly interpolate in-between. The final recommended model becomes:

$$\begin{aligned} R_{(100-x)\%}(\mu_{\text{end}}) &= R_{(100-x)\%}(\mu_c) \\ &\quad + \left(\mathrm{e}^{P_2(\ln|a_c|)} - 1\right)\left[l^{eq}_{(100-x)\%} + a_h\left(\mu_{\text{peak}} - l^{eq}_{(100-x)\%}\right)\right], \\ l^{eq}_{(100-x)\%} &= (\mu_{eq})^{P_{-1;2}(|a_c|)}, \quad \text{for any } a_c \in [-4,-0.01],\ a_h \in [0,1),\ \mu_c \in [1,9] \end{aligned} \tag{4}$$

where the coefficients are found in Table 2.

Table 2. Coefficients needed for the flatline of the IDA softening part in Eq. (4)

	$P_2(y)$ $(y = \ln\|a_c\|)$			$P_{-1;2}(y)$ $(y = \|a_c\|)$		
$(100-x)\% =$	16%	50%	84%	16%	50%	84%
y^{-1}	0	0	0	-0.5111	-0.3817	-0.4118
1	0.2252	0.3720	0.6130	-0.6194	-0.3599	-0.2610
y	-0.1850	-0.3023	-0.4392	0.0928	-0.0019	-0.0070
y^2	0.1039	0.1056	0.0847	0.0163	0.0186	0.0158

As a first, simpler approximation for moderate values of the negative slope a_c, one may assume that in log-space the 16% and 84% flatlines are roughly 30%-lower and 30%-higher than the median, i.e., $R_{(50\pm34)\%}(\mu_{\text{end}}) = R_{50\%}(\mu_{\text{end}})^{1\pm0.3}$.

Fitting the residual part of the IDA

The residual plateau in the SPO is encountered, for example, in braced-frames or fracturing moment-resisting frames. Only limited inspection of such models has appeared in the literature (e.g., Stear and Bea, 1999). The effect of the SPO residual plateau is to "revive" the IDA, allow it to escape the flatline and move on to higher R-values, in an almost linear-system-like fashion, e.g., Fig. 2(c) for $3 < \mu < 5$. We can model this prominent feature by a linear model in the log-space and capture this entire IDA region by a continuous convex curve that smoothly rises from the flatline. This would have been a difficult model, depending on all five backbone parameters, but for the empirical finding that in this region of the IDA, the full quadrilinear model displays virtually the same behavior with an equivalent trilinear (elastic-negative-plateau) model that has the same negative slope a_c, but sports a reduced plateau height of $r_{eq} = r/(1 + a_h(\mu_c - 1))$. Actually, r_{eq} is the residual plateau height of the full model but measured relative to the peak R-value, $R_{\max} = 1 + a_h(\mu_c - 1)$, reached by the SPO (Fig. 3), instead of relative to the yield strength. This revelation leaves us with only two influential parameters, a_c and r_{eq}, resulting in the model:

$$\ln \mu_{x\%} = \beta_{x\%} + \gamma_{x\%} \ln R, \qquad R \in \left(R_{(100-x)\%}(\mu_r), R_{(100-x)\%}(\mu_f)\right] \tag{5}$$
$$\text{where} \quad \beta_{x\%},\, \gamma_{x\%} = P_1(\ln|a_c|) \cdot P_1(\ln r_{eq}),$$
$$\text{for any} \;\; a_c \in [-4, -0.01], \quad r_{eq} \in [0.05, 0.90]$$

where the coefficients can be found in Table 3. An example of this model's application can be seen in Fig. 2(d) for $3 < \mu \leq 5$.

Table 3. Coefficients needed for fitting the IDA residual part in Eq. (5)

	$\beta_{x\%}$			$\gamma_{x\%}$		
$x\% =$	16%	50%	84%	16%	50%	84%
1	-0.3615	0.2391	0.9557	1.1022	1.0846	1.0176
$\ln\|a_c\|$	-0.0729	-0.0297	-0.0696	0.0180	0.0081	0.0203
$\ln r_{eq}$	-0.4557	-0.4907	-0.4759	0.1111	0.1218	0.1086
$\ln r_{eq} \cdot \ln\|a_c\|$	-0.0372	-0.0272	-0.0308	0.0136	0.0086	0.0061

By observing the results, one can derive that the median IDA does behave much like a secant linear segment that takes on smaller slopes as r_{eq} decreases, eventually becoming one with the flatline induced by the negative branch of the SPO. So, by restricting ourselves to (quite practical) ductilities of 10 or less, the modeling could be further simplified if one decides to model the residual branch of the median IDA as a secant by assuming $\gamma_{50\%} = 1$, while generating the 16%, 84% fractiles as a 100%-wide band centered on the median (in the log-space), i.e., $\mu_{(50\pm34)\%}(R) \approx \mu_{50\%}(R)^{1\pm0.5} \approx \beta_{50\%} \cdot R^{1\pm0.5}$. The existing table of $\beta_{50\%}$ coefficients, although not optimal, can still be used for this approximation, since the difference is negligible.

Joining the pieces: The SPO2IDA tool

We have separately modeled the three segments but we have chosen to keep track of only the flattening caused by the negative SPO and the "secant" caused by the residual. To join them

into smooth and continuous curves that accurately resemble the fractile IDAs we need two "filleting curves" that will connect the negative branch flatline to the hardening and the "secant". We can choose to neglect such details and linearly extend all three pieces to a point of mutual interception, which is usually accurate enough. Or we can generate splines through a knot-insertion algorithm (Farin, 1990), which provide a smooth transition from segment to segment, while at the same time offering computational simplicity and robustness, as it preserves convexity and can be made to be monotonic (as the fractile IDAs are). Once this step has been completed, we have an almost complete description of the IDA for any ductility, modeled as an invertible one-to-one function of either μ or R, a choice left to the user as an advantage of the equivalency of the fractiles given R or μ. We are only missing the final flatline, caused by the SPO's ending at ductility μ_f. This can be accurately and easily modeled in the IDAs by adding a flatline at height $R_{(100-x)\%}(\mu_f)$, simultaneously producing the $(100-x)\%$ fractile of global-collapse capacity. By implementing the modeling and joining of segments in software we have generated the SPO2IDA tool, available in a spreadsheet, MATLAB and even as an Internet application (Vamvatsikos, 2001), and does a remarkable job of reproducing the real behavior of oscillators, as demonstrated in Fig. 2(d).

Illustrative Results and Observations

The ease of computation provided by such a tool, plus the unique perspective offered by the IDA-versus-SPO picture, can offer remarkable intuition into the seismic behavior of systems. As a demonstration of the SPO2IDA tool, we present Fig. 4, an array of cases to briefly study the influence of the backbone on the seismic demand and capacity. In each figure we select a basic backbone, vary one or two of its parameters and then generate the median IDA responses and the corresponding global instability collapse-capacities for each case. Fig. 4(a) shows the benefit of delaying the negative branch of the SPO and allowing hardening to reach higher ductilities. Each increase in μ_c allows the median to stay on "equal displacement" longer, proportionally increasing the capacity. On the other hand, in Fig. 4(b), radically changing the hardening slope a_h but keeping an identical negative branch generates an equivalent set of trilinear SPOs, whose capacities only slightly increase with a_h. Actually, the difference in the capacity is small enough to be within the noise in the fitted data, so the resulting capacities are not strictly increasing with a_h. Decreasing the negative slope a_c in Fig. 4(c) has a beneficial effect when no residual plateau is present, as the milder slopes allow higher capacities. Still, if we include an extensive enough residual plateau (Fig. 4(d)), the benefits of the milder slope are restricted to the somewhat lower μ-demands that may influence some earlier limit-states; the global instability collapse capacity is almost the same for all cases, as the backbones have the same r_{eq}, therefore the milder a_c's are providing only a small advantage. Fig. 4(e) shows the benefits of increasing the residual plateau that consequently increases the slope of the "secant" that the IDA follows, thus improving capacities and decreasing the demands. And finally, Fig. 4(f) shows the obvious advantage of allowing higher fracturing ductilities μ_f. The value of μ_f literally decides where to terminate the IDA, at times fully negating the effect of the plateau if it becomes too small; at $\mu_f = 4$ the IDA hardly receives any benefit from the plateau. As intuitive or surprising as some of the pictures in Fig. 4 may be, they are only a glimpse of what our new tool can really do.

On a more practical aspect, note that SPO2IDA can directly produce R-factors and inelastic displacement ratios. The direct mapping of the μ-given-R to the R-given-μ fractiles effortlessly

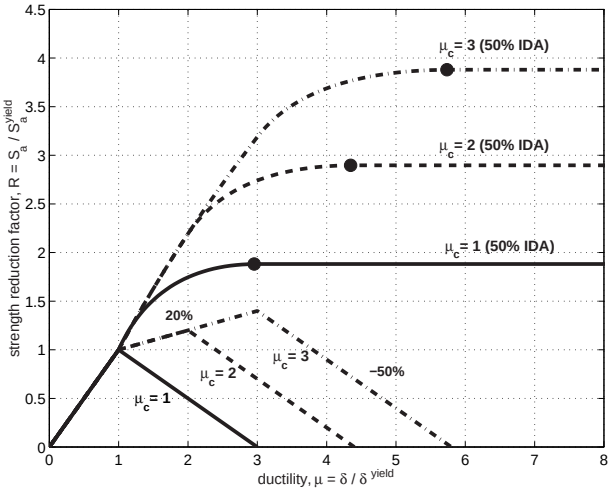

(a) Increasing μ_c helps performance

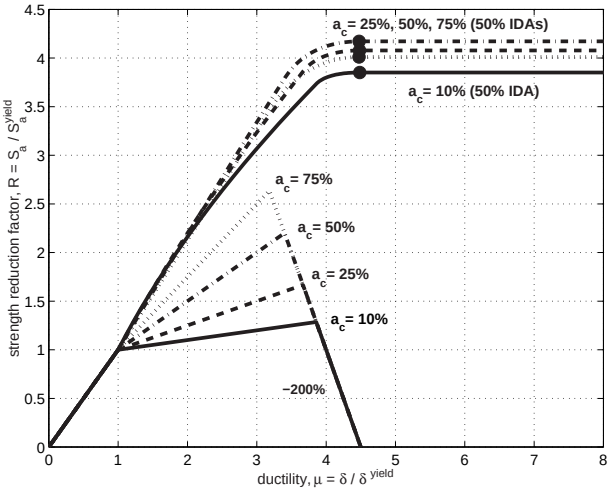

(b) Increasing a_h has negligible effects if same μ_{eq}

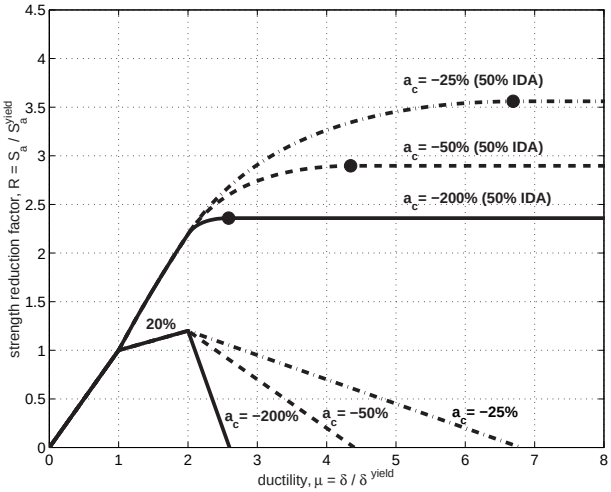

(c) The milder the negative slope, a_c, the better

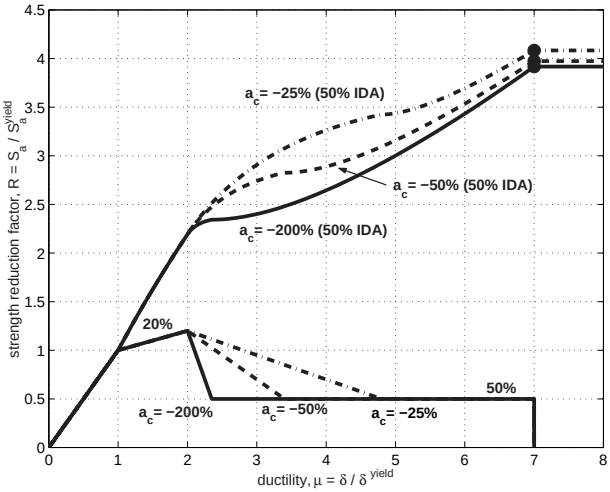

(d) a_c is changing, but constant r_{eq} anchors capacity

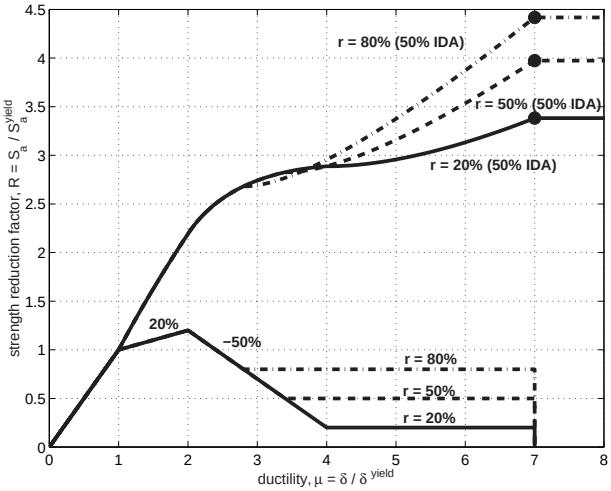

(e) Higher plateau r benefits demand and capacity

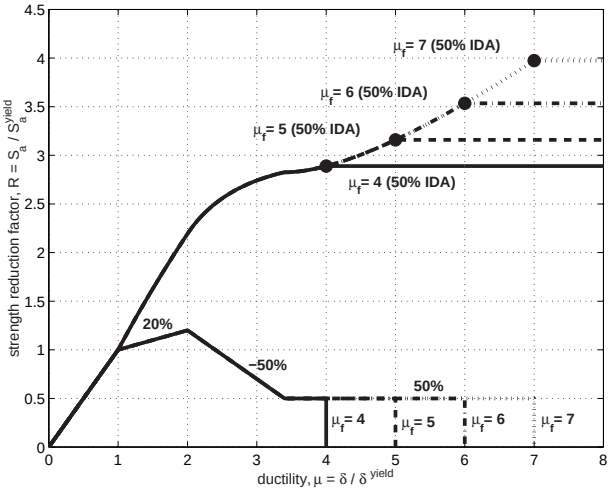

(f) Increasing the fracturing ductility μ_f helps

Figure 4. Demonstrating SPO2IDA: the median demand and capacity as the SPO changes.

provides fractile R-factors. Similarly, one can easily generate fractiles of inelastic displacement ratios, since $(C_\mu)_{x\%} = (C_R)_{x\%} = \mu_{x\%}(R)/R = \mu/R_{(100-x)\%}(\mu)$ (as defined by Miranda, 2001), a feat not possible with models of the average response.

Conclusions

A number of equations have been proposed, defining a flexible tool for performing fast assessments of the demand and capacity of moderate-period SDOF systems with complex backbones. Thus, an engineer-user is able to effortlessly get an accurate, spreadsheet-level estimate of the performance of virtually any such oscillator without having to perform the costly analyses, providing ready insights into the relative advantages and disadvantages of possible design or retrofit alternatives. Finally, by keeping track of both the median and the record-to-record variability, the results can easily be incorporated into modern, probability-based PBEE frameworks.

Acknowledgments

Financial support for this research was provided by the sponsors of the Reliability of Marine Structures Affiliates Program of Stanford University. We would also like to thank Professor H. Krawinkler, L. Ibarra and A. Ayoub for providing the analysis program.

References

Al-Sulaimani, G. J., and J. M. Roessett (1985). Design spectra for degrading systems, *ASCE Journal of Structural Engineering* 111 (12), 127–136.

Farin, G. (1990). *Curves and Surfaces for Computer Aided Geometric Design: A Practical Guide*, 2nd edn., Academic Press, San Diego, CA.

FEMA (1997). NEHRP guidelines for the seismic rehabilitation of buildings, *Report No. FEMA-273*, Federal Emergency Management Agency, Washington DC.

FEMA (2000). Recommended seismic design criteria for new steel moment-frame buildings, *Report No. FEMA-350*, SAC Joint Venture, Federal Emergency Management Agency, Washington DC.

Miranda, E. (2000). Inelastic displacement ratios for structures on firm sites, *ASCE Journal of Structural Engineering* 126 (10), 1150–1159.

Miranda, E. (2001). Estimation of inelastic deformation demands of SDOF systems, *ASCE Journal of Structural Engineering* 127 (9), 1005–1012.

Nassar, A. A., and H. Krawinkler (1991). Seismic demands for SDOF and MDOF systems, *Report No. 95*, The John A.Blume Earthquake Engineering Center, Stanford University, Stanford.

Stear, J. D., and R. G. Bea (1999). A simplified structural analysis method for jacket–type platforms in seismically–active regions, *Report to JIP sponsors*, Dept of Civil & Env Engng, UC Berkeley.

Vamvatsikos, D. (2001). SPO2IDA: Moderate periods. URL `http://tremble.stanford.edu/cgi-bin/spo2ida-mt.pl`

Vamvatsikos, D., and C. A. Cornell (2002a). Incremental dynamic analysis, *Earthquake Engineering and Structural Dynamics* 31 (3), 491–514.

Vamvatsikos, D., and C. A. Cornell (2002b). Seismic performance, capacity and reliability of structures as seen through incremental dynamic analysis, *Report No. RMS-46*, RMS Program, Stanford University, Stanford, (in preparation).